Received: 20 November 2019 | Revised: 18 February 2020 | Accepted: 5 March 2020

DOI: 10.1002/nbm.4298

RESEARCH ARTICLE

NMR IN BIOMEDICINE WILEY

Longitudinal assessment of tissue properties and cardiac diffusion metrics of the ex vivo porcine heart at 7 T: Impact of continuous tissue fixation using formalin

David Lohr[1] | Maxim Terekhov[1] | Franziska Veit[2] | Laura Maria Schreiber[1]

[1]Cellular and Molecular Imaging, Comprehensive Heart Failure Center (CHFC), University Hospital Wuerzburg, Wuerzburg, Germany

[2]Tissue Engineering and Regenerative Medicine (TERM), University Hospital Wuerzburg, Wuerzburg, Germany

Correspondence
David Lohr, Chair of Cellular and Molecular Imaging, Comprehensive Heart Failure Center (CHFC), University Hospital Wuerzburg, Am Schwarzenberg 15, 97078, Wuerzburg, Germany.
Email: e_lohr_d@ukw.de

Funding information
Federal Ministry of Education and Research, Grant/Award Number: 01EO1504

In this study we aimed to assess the effects of continuous formalin fixation on diffusion and relaxation metrics of the ex vivo porcine heart at 7 T. Magnetic resonance imaging was performed on eight piglet hearts using a 7 T whole body system. Hearts were measured fresh within 3 hours of cardiac arrest followed by immersion in 10% neutral buffered formalin. T_2^* and T_2 were assessed using a gradient multi-echo and multi-echo spin echo sequence, respectively. A spin echo and a custom stimulated echo sequence were employed to assess diffusion time-dependent changes in metrics of cardiac diffusion tensor imaging. SNR was determined for b = 0 images. Scans were performed for 5 mm thick apical, midcavity and basal slices (in-plane resolution: 1 mm) and repeated 7, 15, 50, 100 and 200 days postfixation. Eigenvalues of the apparent diffusion coefficient (ADC) and fractional anisotropy (FA) decreased significantly ($P < 0.05$) following fixation. Relative to fresh hearts, FA values 7 and 200 days postfixation were 90% and 80%, while respective relative ADC values at those fixation stages were 78% and 92%. Statistical helix and sheetlet angle distributions as well as respective mean and median values showed no systematic influence of continuous formalin fixation. Similar to changes in the ADC, values for T_2, T_2^* and SNR dropped initially postfixation. Respective relative values compared with fresh hearts at day 7 were 64%, 79% and 68%, whereas continuous fixation restored T_2, T_2^* and SNR leading to relative values of 74%, 100%, and 81% at day 200, respectively. Relaxation parameters and diffusion metrics are significantly altered by continuous formalin fixation. The preservation of microstructure metrics following prolonged fixation is a key finding that may enable future studies of ventricular remodeling in cardiac pathologies.

KEYWORDS
cardiovascular MR methods, diffusion tensor imaging, heart structure, relaxometry

Abbreviations used: |E2A|, absolute sheetlet angle; ADC, apparent diffusion coefficient; cDTI, cardiac diffusion tensor imaging; DTI, diffusion tensor imaging; E2A, secondary eigenvector angle, sheetlet angle; FA, fractional anisotropy; HA, primary eigenvector angle, helix angle; LV, left ventricle; ROI, region of interest; SE, spin echo; SNR, signal-to-noise ratio; STE, stimulated echo; λ_1, primary eigenvalue; λ_2, secondary eigenvalue; λ_3, tertiary eigenvalue.

1 | INTRODUCTION

Cardiac diffusion tensor imaging (cDTI) has become an emerging application in the characterization of cardiac tissue and its functional and structural integrity. It has since been applied in a variety of cardiovascular pathologies, such as hypertrophic[1–3] and dilative cardiomyopathy[3,4] as well as myocardial infarction.[5] In recent years the number of in vivo studies in humans[6–8] and animals[3,9] has increased. But, due to cardiac motion, breath holds, intrinsically low SNR,[10–12] and limited scan times, spatial and angular resolution as well as spatial coverage remain low. Many cardiac studies using DTI have therefore been performed on ex vivo specimens. Usually rapid chemical fixation is applied to prevent autolytic effects after the organ harvest,[13,14] preserving physiological diffusion properties and tissue microstructure as best as possible. This tissue fixation, often performed using formalin, enables long scan times and, thus, ex vivo measurements remain an important scientific tool which provides high resolution and high fidelity, ground truth data. Historically, such data allowed validation of DTI against histology,[9,15–17] proof of concept studies,[18–20] as well as validation of in vivo results.[3,21] Furthermore, cardiac tissue samples can often be gained as a byproduct of other scientific or biomedical studies. The site of cardiac experimentation and fixation, and the site for subsequent DTI measurement may be separated by hundreds of miles.[19] Thus, tissue specimens may be shipped before the MR measurements.

In order to allow an accurate comparison between in vivo and ex vivo measurements it is paramount to assess fixation-induced changes of tissue properties. While there are studies analyzing the impact of tissue fixation on diffusion metrics of the heart,[18,20,22] methodology in studies throughout the years remained highly heterogeneous with regard to the procedure of fixation, storage times and temperature, the fixative itself, and the overall fixation duration.

There is a lack of data on variations of cardiac MRI and DTI parameters following excision of the heart combined with subsequent formalin fixation. For brain tissue, studies have shown that continuous formalin fixation shortens T_1 and T_2 relaxation times compared with the in vivo values[23–29] and that diffusivity is significantly decreased following fixation.[13,30,31]

In a study comparing different fixation methods on the porcine heart, Agger et al[18] concluded that immersion fixation using formalin yielded the diffusion profile most similar to that of "fresh" tissue. In addition, they state that the process of perfusion fixation, in dependence of the perfusion pressure, may possibly inflict tissue damage, resulting in changes of both mean diffusivity and components of the diffusion tensor.

Therefore, the main aim of this study was to assess the impact of formalin immersion fixation on diffusion metrics of the ex vivo porcine heart at 7 T. Diffusion properties for various fixation durations are assessed in dependence of the diffusion time using a stimulated echo diffusion sequence. The secondary aim of this study was to assess fixation-induced alterations in T_2 and T_2^* at ultrahigh field strength and their impact on SNR in diffusion MRI. Results of this study will benefit future ex vivo diffusion experiments regarding fixation, measurement and sequence protocols. In addition, changes in diffusion metrics in dependence of the fixation duration will ease comparison of existing and upcoming studies.

2 | METHODS

2.1 | Porcine heart samples

Hearts (n = 8) were kindly provided by the Translational Center for Regenerative Therapies Wuerzburg, following the animals approved use (55.2 2532–2-256, District Government of Lower Franconia, Germany) in another study. All experiments were performed according to the German Animal Welfare Act and the EU Directive 2010/63/EU. Euthanasia was achieved as described in[32] and hearts were collected, rinsed and stored in physiological saline solution. The eight hearts were harvested in four experiments, where two hearts each were excised with ~20 minutes temporal difference. All samples in this study were harvested from male German Landrace piglets, which were obtained from the same breeder. Body weights ranged from 20-22 kg. Details regarding age and body weight are shown in Table S1.

3 | SAMPLE PREPARATION

Prior to MR measurements and subsequent tissue fixation, both atria were removed, easing the release of air trapped in the ventricles. Sample transport and preparation required ~45–60 minutes before measurement of the first heart (set of two). We always started with MRI measurements of the heart that was excised second, in order to minimize the time differences from excision to measurement between hearts within one set. Hearts were centered in a plastic container filled with physiological saline solution and the sample position was fixed using surgical threads. Directly after the initial MR measurement of the fresh heart, each heart was fixed via immersion in 10% phosphate buffered formalin solution. Before MR measurements of fixed specimens, hearts were briefly (~3-5 minutes) rinsed to remove excess formalin. Throughout the study, hearts were stored immersed in formalin in the scanner operating room. This room is temperature-controlled, allowing storage at a consistent 21 ± 1°C.

3.1 | MRI measurements

3.1.1 | General experimental setup

MRI was performed at bore temperature on a 7 T whole body MRI system (Siemens MAGNETOM Terra, Erlangen, Germany) using a 1/32 Tx/Rx head coil (Nova Medical). Data for the two hearts were acquired in consecutive measurements. Figure 1 shows an illustration of the whole study protocol. Initial measurements on the day of excision were performed on fresh hearts.

For MRI measurements, three short axis slices were positioned in relation to the valves in order to reproduce the slice position in subsequent measurements. The distance between 5 mm slices was set to 15 mm, resulting in single basal, midcavity and apical slices. All scans were performed with an in-plane resolution of 1 mm. Prior to measurements we applied third-order B_0-shimming using the scanner-integrated 3D-shimming algorithm covering the whole three-slice volume. The scan protocol consisted of relaxometry (T_2, T_2^*), diffusion (SE and STE) and SNR (diffusion) measurements. An overview of all sequence parameters is displayed in Table S3. Total acquisition time for the protocol was 63 minutes. Scans for both hearts were therefore completed within 3 hours after excision. Data was postprocessed using MATLAB (MathWorks, Natick, MA) and DSI Studio.[33] Measurements were repeated 7, 15, 50, 100 and 200 days after immersion.

3.1.2 | SNR

In order to evaluate peak SNR in diffusion measurements for the parameters used, we acquired 30 b = 0 images with the spin-echo sequence as well as the stimulated echo sequence (t_{Mix} = 100 ms) for the basal, midcavity and apical slice. Due to a longer diffusion time, the applied spoiler gradients amount to a diffusion weighting of b~18 s/mm^2 in the stimulated echo sequence. Other sequence parameters are described in more detail in the diffusion section below.

3.1.3 | Relaxometry

T_2^* was evaluated based on a 2D multi-gradient-echo sequence with the following imaging parameters, field of view (FOV): 131 mm × 176 mm, number of averages: 8, FA: 30°, bandwidth: 1095 Hz/pixel, TR: 150 ms. Nine echoes per excitation were acquired with TE values distributed between 2.07 and 18.0 ms.

Measurements for T_2 evaluation were performed using a multi-spin-echo spin echo sequence acquiring four averages with bandwidth: 465 Hz/pixel and TR: 2000 ms. Thirty-two images with TE values, distributed equally between 7.5 and 240 ms, were measured. The FOV remained identical with the respective T_2^* acquisition.

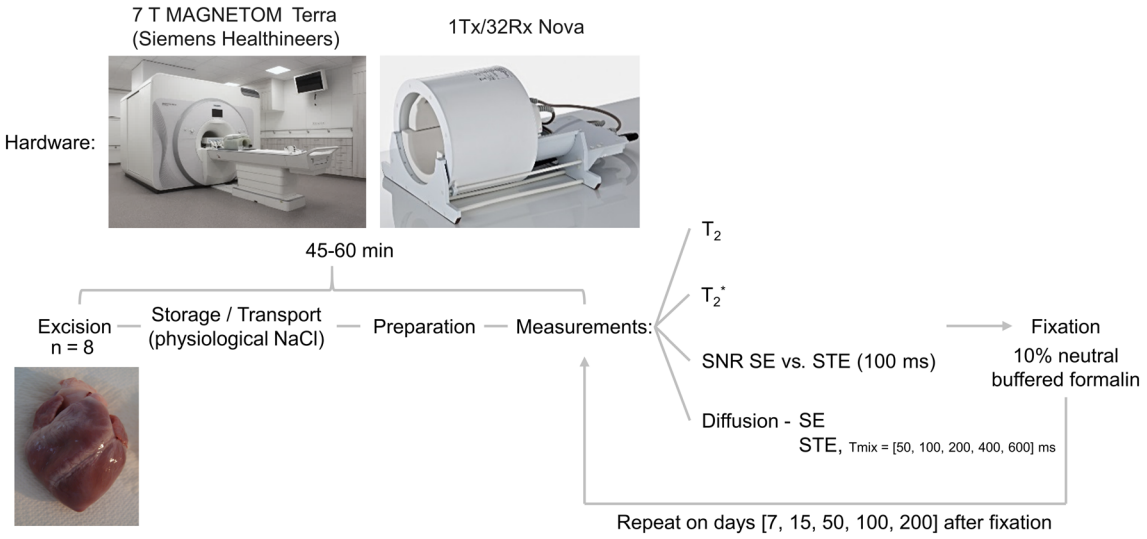

FIGURE 1 Study protocol for the assessment of changes in tissue properties and diffusion metrics in the ex vivo porcine heart due to continuous formalin fixation

3.1.4 | Diffusion

Diffusion data were acquired using a Stejskal-Tanner spin-echo sequence and an in-house written stimulated echo pulse sequence. Both pulse sequences used a monopolar diffusion preparation, EPI readout and a GRAPPA acceleration factor of R = 3. In order to minimize TE we used a bandwidth of 2442 Hz/pixel, leading to a bigger FOV. Further measurement parameters were: TR: 3500 ms, FOV: 208 mm x 256 mm, bandwidth: 2440 Hz/pixel, vendor-supplied diffusion directions (b = 1000 s/mm^2): 6 (averages: 12), reference images (b = 150 s/mm^2): 6 (averages: 12). In order to gain additional information about changes in diffusivity and microstructure, we used varying mixing times (t_{Mix} = 50, 100, 200, 400 and 600 ms) in the stimulated echo sequence, probing diffusion metrics in dependence of the diffusion time. Prolonging the diffusion time allowed shortening of the diffusion gradients, which resulted in shorter echo times. TE for the spin-echo sequence was 44 ms, while TEs for the stimulated echo sequences (t_{Mix}) were 37, 36, 35, 32 and 32 ms.

3.2 | Data processing

All postprocessing was based on DICOM-images created using the vendor's reconstruction pipeline and MATLAB, if not indicated otherwise.

3.2.1 | SNR

Myocardial contours of the left ventricle (LV) were manually segmented and SNR calculated according to the multiple acquisition method.[34] The 30 images were evaluated as a "pseudo" time-dependent dataset, where SNR can be calculated for each voxel (r) using the mean ($\bar{x}$) and standard deviation (σ) over time (t):

$$SNR(r) = \frac{\bar{x}_t(r)}{\sigma_t(r)} \tag{1}$$

The resulting values were averaged for the previously created LV ROI.

In addition, we assessed background noise and SNR in the saline solution as a reference, ensuring coil functionality. As described by Reeder et al[34] noise, assessed in a signal-free area, was corrected for Rayleigh distribution.

3.2.2 | Relaxometry

T_2^* and T_2 maps were reconstructed on a pixel basis using an in-house developed MATLAB script. Here a mono-exponential model fit:

$$S(TE) = S_0 e^{\left(-TE/T_2^*\right)} \tag{2}$$

with the free parameters (T_2^* and S_0) was applied to a preliminary normalized data vector S (TE). T_2 decay was fit the same way. Margins for the fitting parameters of the nonlinear solver were set to 1-50 ms for T_2^* and 1-80 ms for T_2. Providing manually segmented epicardial contours accelerated the fitting process.

3.2.3 | Diffusion

Motion correction was applied in order to correct for eddy current-induced geometrical distortions and DSI Studio[33] was used for reconstruction of the diffusion tensor as described by Jiang et al.[35] All the following processing steps were performed using MATLAB. Eigenvalues (λ_1, λ_2, λ_3), fractional anisotropy (FA) and the apparent diffusion coefficient (ADC) were derived from the diffusion tensor using eigenvalue analysis and the following two equations:

$$FA = \frac{\sqrt{3}}{\sqrt{2}} \frac{\sqrt{(\lambda_1 - \lambda)^2 + (\lambda_2 - \lambda)^2 + (\lambda_3 - \lambda)^2}}{\sqrt{\lambda_1^2 + \lambda_2^2 + \lambda_3^2}} \tag{3}$$

$$ADC = \frac{\lambda_1 + \lambda_2 + \lambda_3}{3} \tag{4}$$

where λ corresponds to the mean eigenvalue of the diffusion tensor.

In addition, we assessed cardiac diffusion metrics such as the primary eigenvector or helix angle (HA) and secondary eigenvector angle (E2A), which correspond to the fiber bundle and sheetlet orientation, respectively. Changes in HA or |E2A| distribution due to fixation were assessed using histograms. Endocardial and epicardial contours of the LV were segmented for subsequent data analysis of diffusion metrics. This also enabled determination of the LV center, which was used to calculate primary and secondary eigenvector angles as described by Ferreira et al.[2] The LV center was recalculated for each time point. Changes in these metrics were also assessed in dependence of the diffusion time up to 600 ms. In order to demonstrate temperature independence, we placed a 20 x 20 pixel ROI in the saline solution for all ADC maps based on the spin echo sequence. This was done for all time points of this study (0, 7, 15, 50, 100, 200 days).

3.2.4 | Statistics

All statistical testing was done using MATLAB. Prior to statistical tests, data were checked for normal distribution using Shapiro–Wilk tests with a significance level of $P < 0.05$. Fixation-induced changes in T_2, T_2^*, eigenvalues of the diffusion tensor, ADC and FA were then assessed using a paired t-test with $P < 0.05$. Bonferroni correction was applied to account for multiple testing.

4 | RESULTS

4.1 | SNR

Figure 2 displays SNR values in the LV in dependence of the tissue fixation duration comparing the spin echo (TE = 44 ms, t_{Mix} = 21 ms) and stimulated echo (TE = 36 ms, t_{Mix} = 100 ms) sequence. For both pulse sequences, the SNR follows a similar trend. There is an initial drop of SNR in the first 7 days of fixation (Δ_{SE}: 32%, Δ_{STE}: 19%) followed by another week of approximately consistent SNR. With longer tissue fixation duration SNR recovers compared with fresh tissue values (Δ_{SE}: 20%, Δ_{STE}: 10%). The use of a stimulated echo approach resulted in a loss of ~33% SNR in the fresh heart. With decreased T_2 and T_2^* this difference was 31% on day 7 after fixation and 25% on day 200 after fixation. Results of the paired t-test are listed in Table S4 and histograms of the SNR distribution are shown in Figure S1. Using the STE sequence resulted in narrower histograms with sharper modes. Destructive B_1 interference, as illustrated in Figure S2, was present in the saline solution in all diffusion scans. Despite this signal variation, the saline SNR reference was consistent throughout this study. In addition, there were no variations in the noise floor.

4.2 | Relaxometry

Representative image contrasts for the varying echo times in T_2^* and T_2 measurements are displayed in Figures S3 and S4 for a midcavity slice of one heart. Alterations of the transverse and the effective transverse relaxation times due to continuous tissue fixation are shown in Figure 3. As visualized by the parameter maps of a representative midcavity slice, both T_2 (see Figure 3A) and T_2^* (see Figure 3B) drop significantly in the first 7 days. Afterwards, we observe slightly increasing values for both T_2 and T_2^*. Mean values of individual hearts as well as their mean ± single standard deviation show that this trend was present in basal, midcavity and apical slices of all hearts. Average values for the initial drop as well as the relative difference after 200 days of continuous fixation are listed in Table 1. On average, T_2 dropped from 49.3 to 32.1 ms (35%) and T_2^* from 25.1 to 19.8 ms (~21%) in the LV in the first 7 days. While T_2^* values almost recovered after 200 days of continuous fixation (<5% mean difference to fresh hearts), T_2 values remain lowered (26% mean difference to fresh hearts). Results of the paired t-test are listed in Table S4.

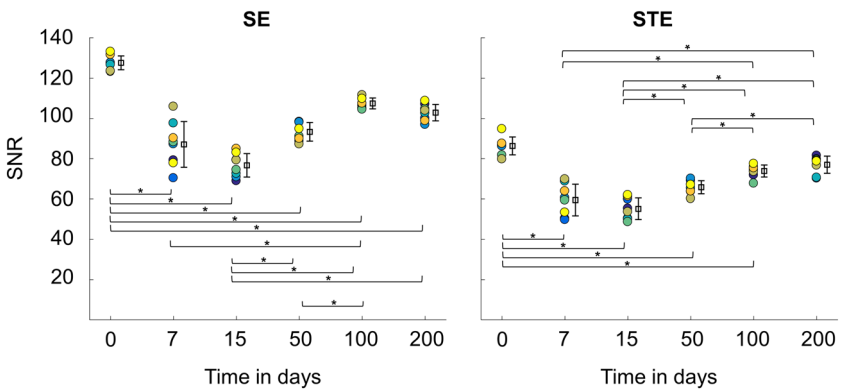

FIGURE 2 SNR in reference scans of the spin echo and stimulated echo (t_{Mix} = 100 ms) sequence for all hearts. Color coding: Hearts 1–8. Displayed are mean values for individual hearts and their mean ± single standard deviation for the different time points prior to and after fixation. Significant differences in paired t-test ($P < 0.05$) are indicated by *

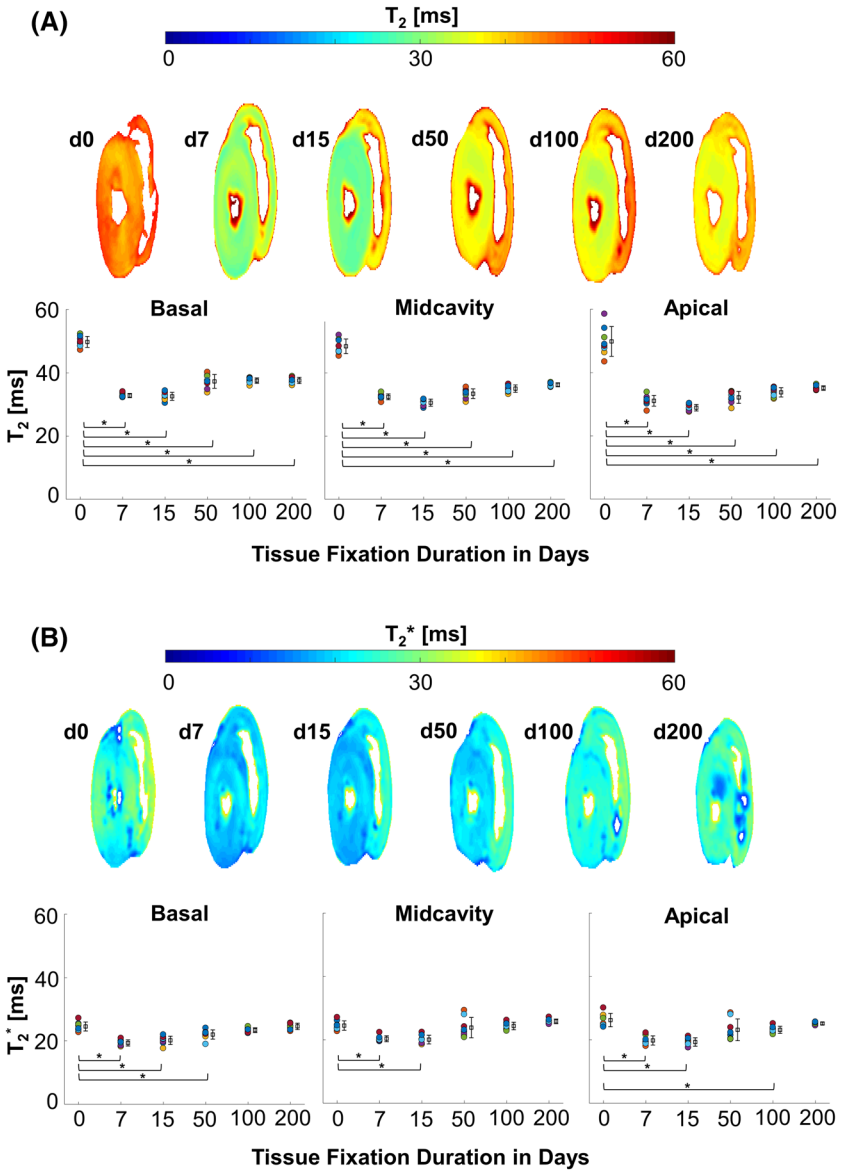

FIGURE 3 T_2 and T_2^* prior to fixation and 7, 15, 50, 100 and 200 days after (A) representative T_2 maps for a single midcavity slice for the different time points prior to and after fixation. Below are mean values for individual hearts and their mean ± single standard deviation. A significant difference in paired t-test ($P < 0.05$) relative to day 0 is indicated by *. Color coding: Hearts 1–8. (B) Corresponding visualization of T_2^*

TABLE 1 Alterations of T_2 and T_2^* due to tissue fixation compared with fresh hearts

	T_2 fresh [ms]	T_2 day-7 [ms]	Δ [%]	T_2 day-200 [ms]	Δ [%]
Apical	49.8 ± 4.7	31.1 ± 1.7	38	35.2 ± 0.7	30
Midcavity	48.3 ± 2.3	32.4 ± 0.9	33	36.3 ± 0.6	25
Basal	49.7 ± 1.7	31.1 ± 0.7	34	37.6 ± 1.0	24
	T_2^* fresh [ms]	T_2^* day-7 [ms]	Δ [%]	T_2^* day-200 [ms]	Δ [%]
Apical	26.2 ± 2.1	19.8 ± 1.5	25	25.1 ± 0.4	4
Midcavity	24.5 ± 1.4	19.3 ± 1.0	21	25.8 ± 0.7	-5
Basal	24.5 ± 1.5	20.3 ± 0.9	17	24.6 ± 1.0	–0.1

4.3 | Diffusion

Mean temporal changes in the eigenvalues of the diffusion tensor, the ADC and FA are shown in Figure 4. All eigenvalues and therefore the ADC decreased, similarly to T_2 and T_2^*, within 7 days following fixation. Changes in λ_2 and λ_3 were rather small. After this initial drop, eigenvalues slightly increased with fixation duration. After 100 days of fixation this led to significant differences compared with first week λ_1 and ADC values.

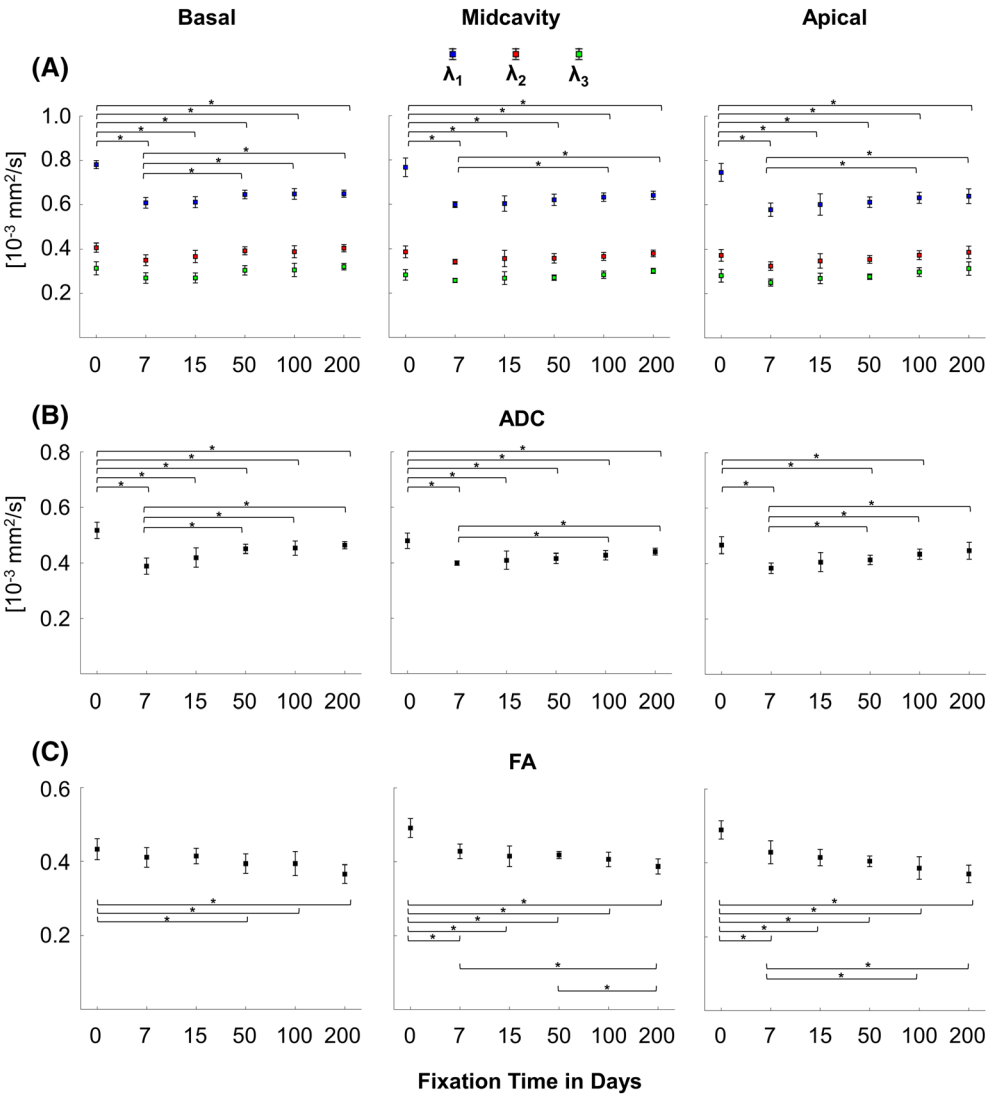

FIGURE 4 Mean ± single standard deviation of diffusion metrics of the left ventricle prior to fixation and 7, 15, 50, 100 and 200 days after fixation for basal, midcavity and apical slices. (A) eigenvalues λ_1 (blue), λ_2 (red), λ_3 (green) of the diffusion tensor. (B) ADC. (C) FA. Standard deviations are of averages across all hearts. A significant difference in paired t-test ($P < 0.05$) is indicated by *. For visibility reasons, test results for the eigenvalues are only shown for λ_1

FA was altered significantly postfixation. However, contrary to the eigenvalue evolution, values decreased with fixation time, leading to significant differences in first week values in midcavity and apical slices after 200 days of fixation. Initial changes in FA due to tissue fixation or tissue fixation duration were smaller and insignificant for basal slices.

Reference values for the ADC are depicted in Figure S5. The average ADC in saline solution was 1.740 ± 0.022 [10^{-3} mm^2/s], with the standard deviation being lower than 2%.

Representative fixation-induced alterations of the main eigenvector orientation and therefore microstructure for heart #5 are displayed in Figure 5. Data were acquired using the spin echo sequence and the diffusion tensor and HA visualized as superquadric glyphs for a basal slice. The expected smooth progression from positive values in the endocardium to negative values in the epicardium is present at all fixation stages. Differences at various fixation stages can be found at the insertion point of the left and right ventricles. Mean HA values (in degrees) for the heart shown in Figure 5 at the time points 0, 7, 15, 50, 100 and 200 days were −1.0°, −0.1°, −2.5°, 2°, −1.6° and 1.25°, respectively. Histograms showing the distribution of HA values for this heart within LV segmentation at different time points after fixation compared with the distribution in unfixed tissue are displayed in Figure S6. There is no systematic shift in the main eigenvector orientation. Respective HA distributions for the remaining seven hearts prior and after 7, 15 and 100 days of fixation are shown in Figure S7. The average standard deviation (over time) in mean values for all hearts was 3.4°.

Figure 6 demonstrates representative variations of the secondary eigenvector orientation for the same basal slice of heart #5. Superquadric glyphs are used to visualize the diffusion tensor and the secondary eigenvector angle (|E2A|). Since the secondary eigenvector orientation is not linked to a certain position in the myocardium, the visual assessment of changes turned out to be difficult compared with the main eigenvector. However, similar to Figure 5, the main difference at different fixation stages was found at the insertion point of the left and right ventricles. While the LV cavity looks similar for scans at days 7, 15, 50, 100 and 200, there is a distinct structural difference compared with day 0. Median |E2A| values (in degrees) for the heart shown in Figure 6 at the time points 0, 7, 15, 50, 100 and 200 days were 64.6°, 64.5°, 65.1°, 65.2°, 64.6° and

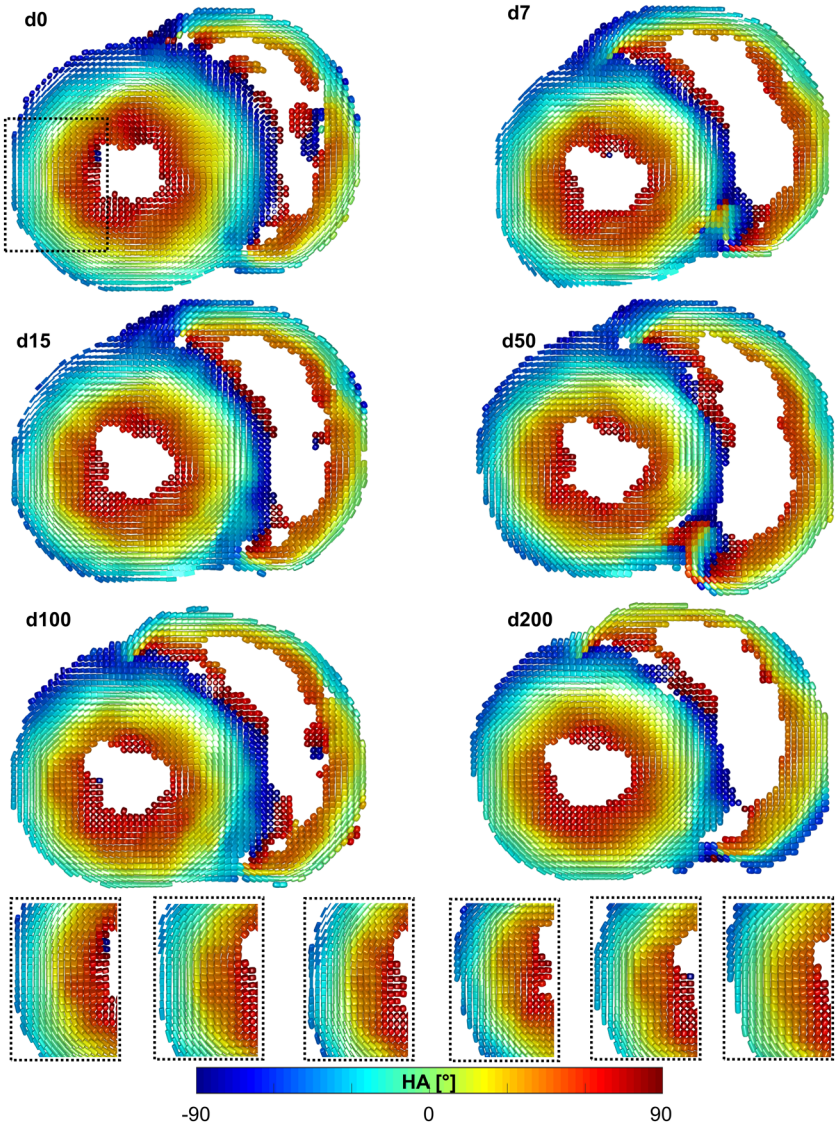

FIGURE 5 Representative helix angle distribution for one heart prior to fixation and 7, 15, 50, 100 and 200 days after fixation. The diffusion tensor for a basal slice is visualized as a superquadric glyph for each pixel. Color-coding of each glyph corresponds to HA values. Dotted line: example section at day 0 and respective zoomed images for the various time points. Threshold for visualization of a pixel as superquadric glyph was set to a FA value of 0.2

64.6°, respectively. Histograms showing the respective |E2A| distribution within LV segmentation at different time points after fixation are presented in Figure S8. |E2A| distributions for the remaining seven hearts prior and after 7, 15 and 100 days of fixation are shown in Figure S9. The average standard deviation (over time) in mean values for all hearts was 6.5°.

Figure 7 shows tissue fixation-induced changes in diffusion metrics (λ_1, λ_2, λ_3, ADC and FA) of the midcavity slice averaged over all eight hearts in dependence of the diffusion time. Values for the diffusion time of 21 ms were acquired using the spin echo sequence. All longer measurements with diffusion times longer than 21 ms were performed using the stimulated echo sequence. Values for individual hearts are displayed in Figure S10.

While λ_1 continually decreased with increasing diffusion time in the unfixed heart, this trend was not apparent after fixation. Values of λ_1 appear rather consistent with increasing diffusion time. As described above, the main eigenvalue of the diffusion tensor drops following fixation. In addition, there is a slight increase with increasing fixation duration. Thus, the difference between λ_1 in fixed and unfixed cardiac tissue is smallest for longer diffusion times and tissue fixation durations (<10%).

Differences of the secondary and tertiary eigenvalues following fixation were small compared with the main eigenvalue. Both λ_2 and λ_3 initially decreased with increasing diffusion time, resulting in a rather consistent state for longer diffusion times (>200 ms). This diffusion time-dependent decrease was highest in unfixed hearts and on average became less impactful for longer tissue fixation durations. ADC curves exhibit the same diffusion time dependency with smaller differences between fixed and unfixed tissue.

FA values increased with increasing diffusion time. This trend was present for all fixation stages and most prominent in the unfixed heart. On average, longer fixation durations led to lower FA values. An initial drop of FA following fixation was present in all hearts.

For all metrics curves reached a plateau between 200 and 400 ms diffusion time.

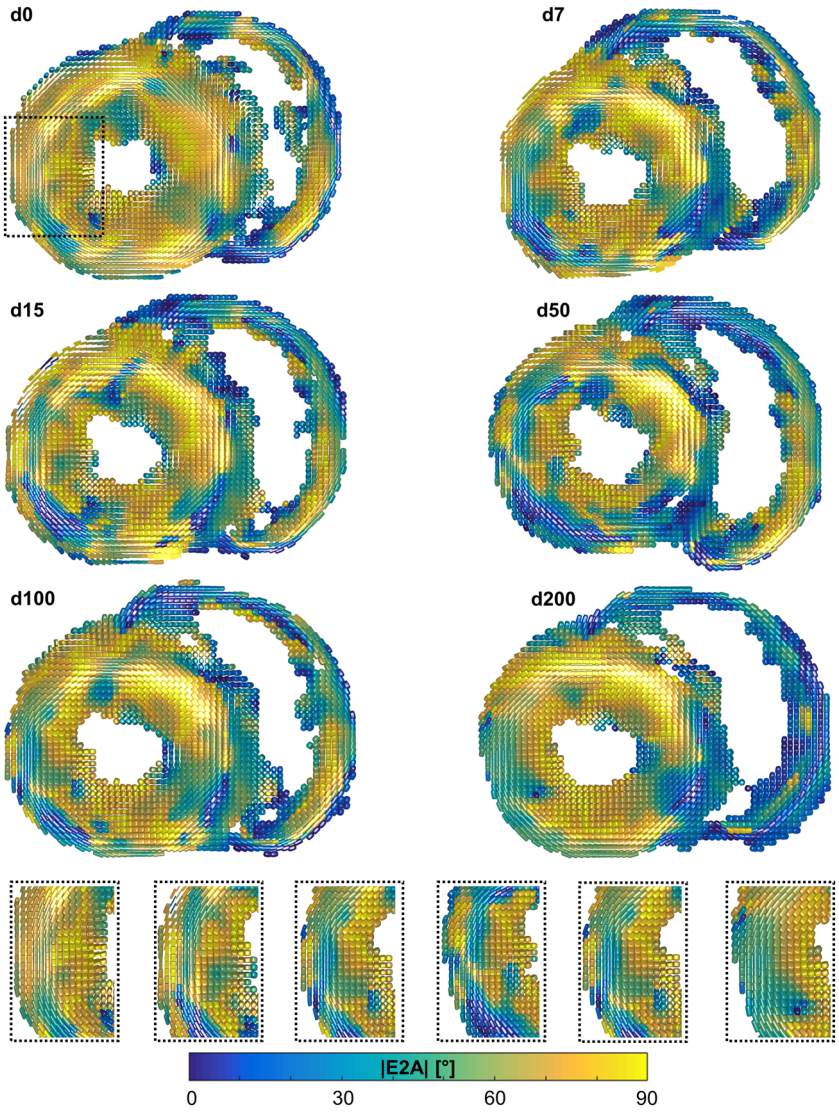

FIGURE 6 Representative secondary eigenvector angle distribution for one heart prior to fixation and 7, 15, 50, 100 and 200 days after fixation. The diffusion tensor for a basal slice is visualized as a superquadric glyph for each pixel. Color-coding of each glyph corresponds to |E2A| values. Dotted line: example section at day 0 and respective zoomed images for the various time points. Threshold for visualization of a pixel as superquadric glyph was set to a FA value of 0.2

5 | DISCUSSION

We have demonstrated tissue fixation and fixation duration-dependent alterations of various MRI (T_2, T_2^*, SNR) and diffusion metrics (ADC, λ_1, λ_2, λ_3, FA, HA, |E2A|) in the LV of the porcine heart at 7 T. Our results show that T_2 and T_2^* relaxation times were continuously altered by immersion fixation in formalin and that SNR values strongly correlated with the respective changes in T_2 and T_2^*. In addition, we found that tissue fixation significantly changed the main eigenvalue of the diffusion tensor, ADC and FA, and that continuous changes in the main eigenvalues, ADC and FA after a fixation duration of 15 days were not significant. By contrast, no systematic changes in structural parameters, such as HA and |E2A|, were introduced by fixation, independent of the immersion duration. This is an important finding for studies assessing ventricular remodeling of cardiac microstructure in various cardiac pathologies.

SNR in diffusion MRI directly influences the data fidelity[11,12] of derived diffusion parameters. Most ex vivo studies use a Stejskal-Tanner diffusion preparation and EPI readout. Thus, SNR strongly depends on both T_2 and T_2^*. Since ex vivo studies are usually performed to achieve high quality and high fidelity data, study protocols should be optimized with respect to SNR. Our results show that SNR decreases (mean: ~32%) initially after tissue fixation and that SNR was somewhat restored (mean: ~20%) with prolonged tissue fixation. This change in SNR is mainly due to the changes observed in T_2 and T_2^* relative to the used echo times as well as subsequent k-space filter effects. Special care needs to be taken in order to avoid further reduction of T_2^* due to increased B_0 inhomogeneity at ultrahigh field strengths (≥7 T).

Many studies have reported a decrease in T_2 in nervous tissue or other organs following tissue fixation using formalin.[23–29] To our knowledge such changes in relaxation parameters have not been yet reported for the heart. Initial T_2 changes following tissue fixation observed in this study fit well to the literature values for brain tissue listed above. T_2 shortening in nervous tissue has been described in many studies and has been attributed to multiple causes, such as increased tissue rigidity due to protein cross-linking, interactions of water molecules and myelin lipids in

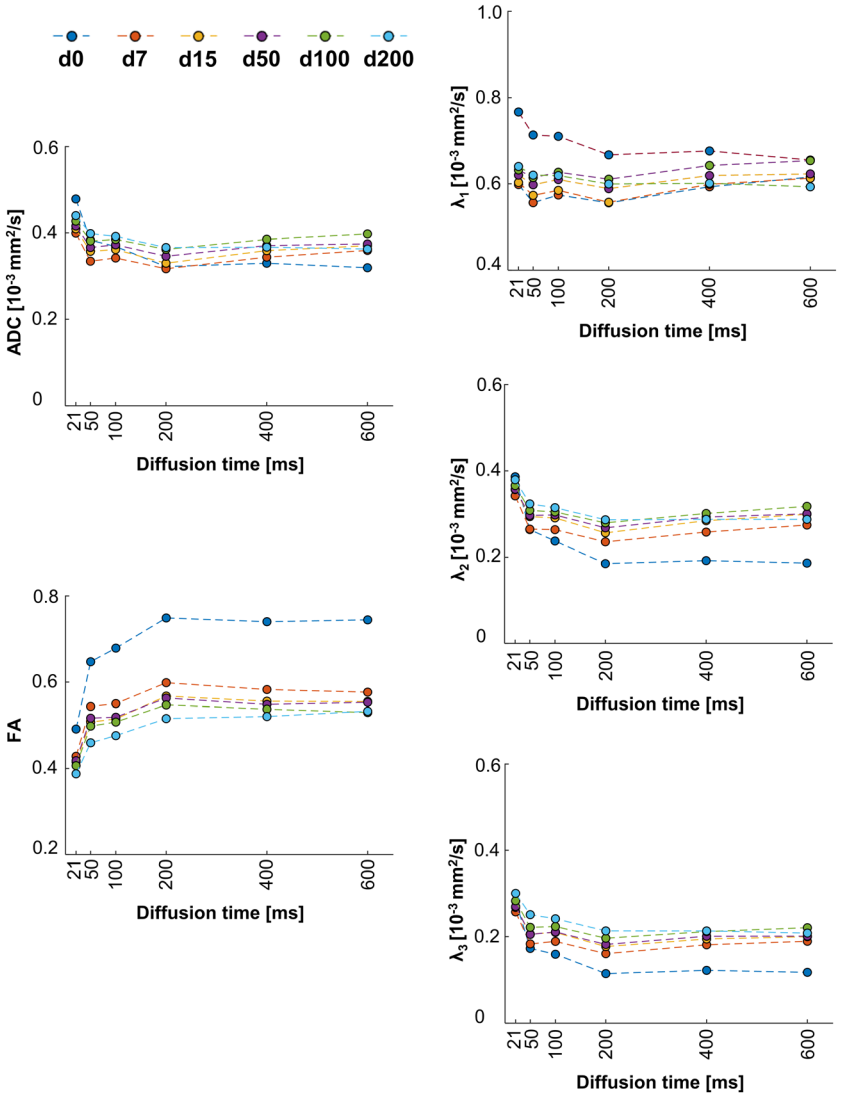

FIGURE 7 Average diffusion time-dependent changes of λ_1, λ_2, λ_3, ADC and FA in the midcavity slice in dependence of the fixation duration

tissue compartments,[36] changes in diffusion rates,[37] intra/extra-cellular water components,[25] tissue dehydration[28,38] and regular replacements of formalin solution.[27] The analysis of the mechanisms of T_2 shortening and their application to heart tissue was outside the scope of this study.

We rather focused on changes in MR and diffusion metrics induced by continuous tissue fixation in order to (1) ease optimization of future study protocols and (2) enable comparisons of past and future studies regarding fixed versus unfixed tissue, fixation duration, and spin echo versus stimulated echo data.

Dawe et al[23] reported a gradual increase (20%, 60-90 days postmortem) of T_2 values in "deep" brain tissue for longer fixation durations, following the initial decrease after formalin immersion. We observed an increase (~13%) in T_2 between 15 and 50 days of fixation. Dawe et al[23] argue that this recovery in T_2 values is connected to latent tissue decomposition.

In our study, we removed the atria from all hearts in order to ease the removal of trapped air and fixative distribution, allowing penetration of the myocardial wall from both sides. Aldehyde fixation penetration occurs with a rate of 0.5 to 1 mm/hour at room temperature and we observed the pale yellow color change, which indicates penetration, shortly after immersion. Multiple studies have shown that autolytic effects on cardiac tissue are very slow.[14,32,39] It is therefore unlikely that the gradual increase in T_2 at later stages of fixation is related to latent effects of tissue decomposition. During the fixation process cells move through stages of (1) shrinkage, (2) prolonged swelling and (3) secondary shrinkage. As mentioned above, changes in T_2 have been attributed to changes in intra- and extra-cellular volume components.[25] In this study we apply formalin, a neutral buffered, aqueous solution of formaldehyde (systematic name: methanal), with a formaldehyde concentration of 4%. Formaldehyde concentrations below 5% only cause very minimal initial shrinkage followed by extensive swelling[40] and later on shrinkage. Observed decreases and increases in T_2 may thus be caused by cell swelling and shrinkage, respectively. A dedicated study resolving the fixation process itself will be necessary to completely exclude influences of tissue decomposition and variations in both heart size and contraction state. In addition to SNR, alterations in T_2 may possibly change T_2 weightings in the diffusion-weighted images acquired.

Since we did not observe any interference patterns in images for T_2 quantification due to imperfect inversions, normalized the signal-time curves and checked for mono-exponential decay via goodness of fit, we believe that B_1 imperfections did not lead to first-order approximation errors in measured T_2 values. In addition, the goodness of fit showed that the effect of B_1 inhomogeneity on SNR was negligible for the analyzed tissue.

With 0.62 ± 0.1 (10^{-3} mm^2/s), our ADC values in this study are in good agreement with our previous work at 7 T[32] (0.51-0.66 [10^{-3} mm^2/s]) using fresh hearts from animals of the same breed and comparable weight. ADC values of fresh hearts reported by Mazumder et al[20] (0.52 ± 0.026 [10^{-3} mm^2/s], Yorkshire, 41-50 kg) and Agger et al[18] (0.54 ± 0.026 [10^{-3} mm^2/s], Danish Landrace, 50-60 kg) are slightly lower and ADC values of fixed hearts reported by Wu et al[41] (0.671 ± 0.106 [10^{-3} mm^2/s], minipigs, 45-50 kg) and Pashakhanloo et al[42] (0.633 ± 0.04 [10^{-3} mm^2/s], Yorkshire, 50 ± 18 kg) are slightly higher. Literature results of comparisons between fixed and unfixed heart tissue are sparse. While the ADC in our study decreases after fixation, Agger et al[18] report only a slight increase (11%) and Mazumder et al[20] a strong increase in the ADC (~54%). There are contradictory literature reports on postfixation ADC as well. While Shepherd et al[26] report an increase in ADC, others have shown a decrease postfixation.[13,31,43] These contradictory reports may possibly be the result of varying tissue storage conditions during sample preparation.

In their study on the effects of various fixation methods on heart tissue, Agger et al[18] showed that freezing of heart tissue leads to large increases in the ADC (71%) and that subsequent perfusion fixation will further increase the ADC (88%). Due to limited scanner availability, Mazumder et al[20] stored freshly excised hearts in an ice bath for a prolonged period of time (5-48 h) in order to prevent tissue decomposition prior to scans, while Shepherd el al[26] placed excised rat brains in ice-cold artificial cerebrospinal fluid for 1 h in order to minimize ischemic damage. None of the studies reporting reduced ADC values have used ice, ice baths, or temperatures below 4°C for storage. A dedicated study may help to assess the influence of ice or varying storage temperatures on various tissue types, but this has not been the scope of our study.

There is more consensus in studies regarding the effect of formalin fixation on FA. Comparisons of prefixation and postfixation tissue (heart and nervous tissue) report consistent or decreasing FA following fixation. The results in our study are in good agreement with Agger et al[18] and Mazumder et al,[20] who scanned hearts prefixation and postfixation with a time difference of 24 hours and 12-18 days, respectively. We show that FA decreases with prolonged tissue fixation. This may explain why Agger et al[18] reported consistent FA values, while Mazumder et al[20] reported a decrease in FA.

Our results show that all eigenvalues decrease following fixation. Alterations of the main eigenvector of diffusion are the most pronounced, and the second and third eigenvalues are less affected. Both Agger et al,[18] for heart tissue, and D'Arceuil and de Crespigny,[13] for white matter, showed that the effects on the main eigenvector are most pronounced. In order to improve our understanding of changes in the ADC and FA it is paramount to report changes in the individual eigenvalues. Future studies analyzing diffusion metrics in highly structured tissue, such as the brain or the heart, should therefore report all eigenvalues.

Agger et al[18] demonstrated that immersion fixation using formalin does not affect main fiber orientation and therefore tractography results. This is in agreement with studies by Scollan et al[16] and Helm et al,[44] who compared the main eigenvector orientation in fixed hearts to myofiber orientation in histology. Results obtained in this study support this observation. Even prolonged, continuous tissue fixation had little impact on the helix angle and therefore main eigenvector orientation. Furthermore, the smooth gradient from endocardium to epicardium was consistent in the presence of scan-to-scan slice offsets.

To our knowledge this is the first study analyzing effects of formalin fixation on the secondary eigenvector orientation within cardiac tissue. Recent developments in cardiac DTI, particularly in vivo applications, have shown that the secondary eigenvector angle holds high diagnostic value for myocardial remodeling in cardiac pathologies.[2–4] In this study we demonstrate that continuous tissue fixation using formalin does not affect the average secondary eigenvector orientation. Sheetlets generally run perpendicular to myocytes, which means through-plane in the short axis slice, and thus scan-to-scan slice offsets are more apparent in the visualization of |E2A|.

Kim et al[45] report a consistent main eigenvalue and decreasing secondary and tertiary eigenvalues for increasing diffusion times in refrigerated and thawed heart tissue of the calf. While this is in good agreement with the changes we found in heart tissue postfixation, we also found that diffusion time-induced alterations in fixed and unfixed tissue follow a similar trend, but with a different scale. Longer diffusion times and therefore increased anisotropy have been shown to decrease uncertainty in the determination of the main eigenvector orientation.[46] In this study we have shown that the dependence of FA from diffusion encoding time is reduced following fixation using formalin, indicating that formalin fixation introduces diffusion barriers along the main direction of diffusion.

Reference values, such as SNR in the saline solution and noise in the background, were meant to remove external factors, such as temperature and coil heating, for the assessment of SNR and diffusion metrics. While the background noise was very stable, SNR in the saline solution was affected by destructive B_1 interference. However, considering the combination of the SNR and the ADC reference in saline solution, we believe that the results of this study are unaffected by temperature variation.

In order to minimize tissue decomposition-induced changes in derived metrics of fresh hearts, we set the scanning protocol to 63 minutes, trading higher SNR for limited volume coverage. The diffusion weighting of b = 1000 s/mm^2 was chosen to maintain comparability to other fixation studies on porcine hearts such as Agger et al[18] (b = 1000 s/mm^2) and Mazumder et al[20] (1271 s/mm^2). While additional higher b-values may

have increased the dynamic range for restricted diffusion and enabled analysis based on non-Gaussian models, they also require longer diffusion gradients, leading to longer echo times and a loss in SNR, particularly at 7 T. In this study we show that fixation leads to decreases in T_2 and T_2^*, which are already short at ultrahigh field strengths. An assessment of respective tradeoffs and optimal b-values for ex vivo cDTI of fixed porcine hearts at 7 T may be subject to future studies.

Since we received sets of two hearts per experiment, prefixation scans within one set were performed with a time difference of ~40 minutes between excision and measurement. We found no systematic difference in diffusivity between hearts measured first and second. This is in agreement with prior experiments analyzing sample stability of fresh hearts following excision.[32] However, variations in heart size and times for transport, tissue preparation and sample fixation may have resulted in different tissue temperatures. Thus, prefixation scans in this study may therefore include a temperature bias.

Throughout the study, hearts were repeatedly taken from the fixation container and placed in dedicated plastic containers for measurements. Therefore, slight offsets in slice positioning were present in some repeat scans, despite slice positioning with respect to anatomical markers. In general these offsets were more pronounced for the prefixation scans and rather small for scans of fixed hearts. They may thus be related to tissue changes introduced by the fixation process. While these offsets had little impact on derived structural parameters in the LV of fixed samples, there were distinct differences at intersection points to the right ventricle. Particularly at very basal slices, structural coherence at these points was lower. Further analysis of these changes may be part of future studies, but was outside the scope of this work.

In conclusion, we have demonstrated that continuous immersion fixation of porcine hearts using formalin leads to alterations of relaxation parameters and diffusion metrics, such as eigenvalues, ADC and FA. Thus, tissue fixation durations should be kept in mind when interpreting the impact of diseases on these parameters. In addition, our results highlight the importance of proper method selection and reproducible tissue handling, preparation and storage. In recent years, metrics of microstructure been shown to be precise and specific markers for remodeling in cardiac pathologies.[3–5,19] The preservation of anisotropy and overall microstructure following even long periods of immersion in formalin may enable future studies assessing ventricular remodeling of cardiac microstructure in various cardiac pathologies in more detail.

ACKNOWLEDGEMENTS

The authors thank Mihaela Pali for excellent surgical assistance.

Parts of this work will be used in the doctoral thesis of David Lohr.

FUNDING INFORMATION

This work was supported by the Federal Ministry of Education and Research (grant number, 01EO1504).

ORCID

David Lohr https://orcid.org/0000-0002-6509-3776

REFERENCES

1. Ariga R, Tunnicliffe EM, Manohar SG, et al. Identification of myocardial disarray in patients with hypertrophic cardiomyopathy and ventricular arrhythmias. *J Am Coll Cardiol*. 2019;73(20):2493-2502.
2. Ferreira PF, Kilner PJ, McGill LA, et al. In vivo cardiovascular magnetic resonance diffusion tensor imaging shows evidence of abnormal myocardial laminar orientations and mobility in hypertrophic cardiomyopathy. *J Cardiovasc Magn Reson*. 2014;16(1):87. https://doi.org/10.1186/s12968-014-0087-8
3. Nielles-Vallespin S, Khalique Z, Ferreira PF, et al. Assessment of myocardial microstructural dynamics by in vivo diffusion tensor cardiac magnetic resonance. *J Am Coll Cardiol*. 2017;69(6):661-676.
4. von Deuster C, Sammut E, Asner L, et al. Studying dynamic myofiber aggregate reorientation in dilated cardiomyopathy using in vivo magnetic resonance diffusion tensor imaging. *Circ Cardiovasc Imaging*. 2016;9(10):e005018. https://doi.org/10.1161/CIRCIMAGING.116.005018
5. Mekkaoui C, Jackowski MP, Kostis WJ, et al. Myocardial scar delineation using diffusion tensor magnetic resonance tractography. *J Am Heart Assoc*. 2018;7(3):e007834. https://doi.org/10.1161/JAHA.117.007834
6. Mekkaoui C, Reese TG, Jackowski MP, et al. Diffusion tractography of the entire left ventricle by using free-breathing accelerated simultaneous multisection imaging. *Radiology*. 2017;282(3):850-856.
7. Nguyen C, Fan Z, Sharif B, et al. In vivo three-dimensional high resolution cardiac diffusion-weighted MRI: A motion compensated diffusion-prepared balanced steady-state free precession approach. *Magn Reson Med*. 2014;72(5):1257-1267.
8. Stoeck CT, von Deuster C, Genet M, Atkinson D, Kozerke S. Second order motion compensated spin-echo diffusion tensor imaging of the human heart. *Magn Reson Med*. 2016;75(4):1669-1676.
9. Sosnovik DE, Mekkaoui C, Huang S, et al. Microstructural impact of ischemia and bone marrow-derived cell therapy revealed with diffusion tensor magnetic resonance imaging tractography of the heart in vivo. *Circulation*. 2014;129(17):1731-1741.
10. Landman BA, Farrell JA, Huang H, Prince JL, Mori S. Diffusion tensor imaging at low SNR: nonmonotonic behaviors of tensor contrasts. *Magn Reson Imaging*. 2008;26(6):790-800.

11. Scott AD, Nielles-Vallespin S, Ferreira PF, McGill L-A, Pennell DJ, Firmin DN. The effects of noise in cardiac diffusion tensor imaging and the benefits of averaging complex data. *NMR Biomed*. 2016;29(5):588-599.
12. McClymont D, Teh I, Schneider JE. The impact of signal-to-noise ratio, diffusion-weighted directions and image resolution in cardiac diffusion tensor imaging – insights from the ex-vivo rat heart. *J Cardiovasc Magn Reson*. 2017;19(1):90. https://doi.org/10.1186/s12968-017-0395-x
13. D'Arceuil H, de Crespigny A. The effects of brain tissue decomposition on diffusion tensor imaging and tractography. *Neuroimage*. 2007;36(1):64-68.
14. Eggen MD, Swingen CM, Iaizzo PA. Ex vivo diffusion tensor MRI of human hearts: Relative effects of specimen decomposition. *Magn Reson Med*. 2012;67(6):1703-1709.
15. Hsu EW, Muzikant AL, Matulevicius SA, Penland RC, Henriquez CS. Magnetic resonance myocardial fiber-orientation mapping with direct histological correlation. *Am J Physiol Heart Circ Physiol*. 1998;274(5):H1627-H1634.
16. Scollan DF, Holmes A, Winslow R, Forder J. Histological validation of myocardial microstructure obtained from diffusion tensor magnetic resonance imaging. *Am J Physiol Heart Circ Physiol*. 1998;275(6):H2308-H2318.
17. Sosnovik DE, Wang R, Dai G, et al. Diffusion spectrum MRI tractography reveals the presence of a complex network of residual myofibers in infarcted myocardium. *Circ Cardiovasc Imaging*. 2009;2(3):206-212.
18. Agger P, Lass T, Smerup M, Frandsen J, Pedersen M. Optimal preservation of porcine cardiac tissue prior to diffusion tensor magnetic resonance imaging. *J Anat*. 2015;227(5):695-701.
19. Beyhoff N, Lohr D, Foryst-Ludwig A, et al. Characterization of myocardial microstructure and function in an experimental model of isolated subendocardial damage. *Hypertension*. 2019;74(2):295-304.
20. Mazumder R, Choi S, Clymer BD, White RD, Kolipaka A. Diffusion tensor imaging of healthy and infarcted porcine hearts: study on the impact of formalin fixation. *J Med Imag Rad Sci*. 2016;47(1):74-85.
21. Abdullah OM, Drakos SG, Diakos NA, Wever-Pinzon O, Kfoury AG, Stehlik J. Characterization of diffuse fibrosis in the failing human heart via diffusion tensor imaging and quantitative histological validation. *NMR Biomed*. 2014;27(11):1378-1386.
22. Giannakidis A, Gullberg GT, Pennell DJ, Firmin DN. Value of formalin fixation for the prolonged preservation of rodent myocardial microanatomical organization: evidence by MR diffusion tensor imaging. *Anat Rec*. 2016;299(7):878-887.
23. Dawe RJ, Bennett DA, Schneider JA, Vasireddi SK, Arfanakis K. Postmortem MRI of human brain hemispheres: T2 relaxation times during formaldehyde fixation. *Magn Reson Med*. 2009;61(4):810-818.
24. Nagara H, Inoue T, Koga T, Kitaguchi T, Tateishi J, Goto I. Formalin fixed brains are useful for magnetic resonance imaging (MRI) study. *J Neurol Sci*. 1987;81(1):67-77.
25. Shatil AS, Uddin MN, Matsuda KM, Figley CR. Quantitative ex vivo MRI changes due to progressive formalin fixation in whole human brain specimens: longitudinal characterization of diffusion, relaxometry, and myelin water fraction measurements at 3T. *Front Med*. 2018;5:31. https://doi.org/10.3389/fmed.2018.00031
26. Shepherd TM, Thelwall PE, Stanisz GJ, Blackband SJ. Aldehyde fixative solutions alter the water relaxation and diffusion properties of nervous tissue. *Magn Reson Med*. 2009;62(1):26-34.
27. Thickman DI, Kundel HL, Wolf G. Nuclear magnetic resonance characteristics of fresh and fixed tissue: the effect of elapsed time. *Radiology*. 1983;148(1):183-185.
28. Tovi M, Ericsson A. Measurements of T1 and T2 over time in formalin-fixed human whole-brain specimens. *Acta Radiol*. 1992;33(5):400-404.
29. Yong-Hing CJ, Obenaus A, Stryker R, Tong K, Sarty GE. Magnetic resonance imaging and mathematical modeling of progressive formalin fixation of the human brain. *Magn Reson Med*. 2005;54(2):324-332.
30. Wang C, Song L, Zhang R, Gao F. Impact of fixation, coil, and number of excitations on diffusion tensor imaging of rat brains at 7.0 T. *Eur Radiol Exper*. 2018;2(1):25. https://doi.org/10.1186/s41747-018-0057-2
31. Pattany PM, Puckett WR, Klose KJ, et al. High-resolution diffusion-weighted MR of fresh and fixed cat spinal cords: evaluation of diffusion coefficients and anisotropy. *Am J Neuroradiol*. 1997;18(6):1049-1056.
32. Lohr D, Terekhov M, Weng AM, Schroeder A, Walles H, Schreiber LM. Spin echo based cardiac diffusion imaging at 7T: An ex vivo study of the porcine heart at 7T and 3T. *PLoS ONE*. 2019;14(3):e0213994. https://doi.org/10.1371/journal.pone.0213994
33. Yeh F-C. DSI Studio. http://dsi-studio.labsolver.org. Accessed April 22, 2016.
34. Reeder SB, Wintersperger BJ, Dietrich O, et al. Practical approaches to the evaluation of signal-to-noise ratio performance with parallel imaging: Application with cardiac imaging and a 32-channel cardiac coil. *Magn Reson Med*. 2005;54(3):748-754.
35. Jiang H, van Zijl PC, Kim J, Pearlson GD, Mori S. DtiStudio: resource program for diffusion tensor computation and fiber bundle tracking. *Comput Methods Programs Biomed*. 2006;81(2):106-116.
36. Laule C, Vavasour IM, Kolind SH, et al. Magnetic resonance imaging of myelin. *Neurotherapeutics*. 2007;4(3):460-484.
37. Bottomley PA, Foster TH, Argersinger RE, Pfeifer LM. A review of normal tissue hydrogen NMR relaxation times and relaxation mechanisms from 1–100 MHz: Dependence on tissue type, NMR frequency, temperature, species, excision, and age. *Med Phys*. 1984;11(4):425-448.
38. Shepherd TM, Flint JJ, Thelwall PE, et al. Postmortem interval alters the water relaxation and diffusion properties of rat nervous tissue--implications for MRI studies of human autopsy samples. *Neuroimage*. 2009;44(3):820-826.
39. Schmid P, Lunkenheimer PP, Redmann K, et al. Statistical analysis of the angle of intrusion of porcine ventricular myocytes from epicardium to endocardium using diffusion tensor magnetic resonance imaging. *Anat Rec*. 2007;290(11):1413-1423.
40. Crawford CNC, Barer R. The action of formaldehyde on living cells as studied by phase-contrast microscopy. *Q J Microsc Sci*. 1951;s3–92(20):403-452.
41. Wu EX, Wu Y, NichollsJM, et al. MR diffusion tensor imaging study of postinfarct myocardium structural remodeling in a porcine model. *Magnetic resonance in medicine*. 2007;58(4):687-695.
42. Pashakhanloo F, Herzka DA, Mori S, et al. Submillimeter diffusion tensor imaging and late gadolinium enhancement cardiovascular magnetic resonance of chronic myocardial infarction. *Journal of cardiovascular magnetic resonance : official journal of the Society for Cardiovascular Magnetic Resonance*. 2017;19(1):9.
43. Madi S, Hasan KM, Narayana PA. Diffusion tensor imaging of in vivo and excised rat spinal cord at 7 T with an icosahedral encoding scheme. *Magn Reson Med*. 2005;53(1):118-125.

44. Helm PA, Younes L, Beg MF, Ennis DB, Leclercq C, Faris OP. Evidence of structural remodeling in the dyssynchronous failing heart. *Circ Res*. 2006; 98(1):125-132.
45. Kim S, Chi-Fishman G, Barnett AS, Pierpaoli C. Dependence on diffusion time of apparent diffusion tensor of ex vivo calf tongue and heart. *Magn Reson Med*. 2005;54(6):1387-1396.
46. Jones DK. Determining and visualizing uncertainty in estimates of fiber orientation from diffusion tensor MRI. *Magn Reson Med*. 2003;49(1):7-12.

SUPPORTING INFORMATION

Additional supporting information may be found online in the Supporting Information section at the end of this article.

How to cite this article: Lohr D, Terekhov M, Veit F, Schreiber LM. Longitudinal assessment of tissue properties and cardiac diffusion metrics of the ex vivo porcine heart at 7 T: Impact of continuous tissue fixation using formalin. *NMR in Biomedicine*. 2020;33:e4298. https://doi.org/10.1002/nbm.4298